X-ray computed tomography used to measure fiber orientation in CFRP laminates

Akinori Yoshimura [1,*], Ryohei Hosoya [2], Jun Koyanagi [3], Toshio Ogasawara [1]

[1] *Advanced Composite Research Center, Institute of Aeronautical Technology, Japan Aerospace Exploration Agency (JAXA), 6-13-1 Osawa, Mitaka, Tokyo 181-0015, JAPAN*

[2] *Graduate School of Industrial Science and Technology, Tokyo University of Science, 6-3-1 Niijuku, Katsushika-ku, Tokyo 125-8585, JAPAN*

[3] *Department of Materials Science and Technology, Tokyo University of Science, 6-3-1 Niijuku, Katsushika-ku, Tokyo 125-8585, JAPAN*

*Corresponding author

6-13-1 Osawa, Mitaka, Tokyo 181-0015, JAPAN

Tel.: +81 50 3362 7349

E-mail: yoshimura.akinori@jaxa.jp

X-ray computed tomography used to measure fiber orientation in CFRP laminates

This paper explains a new method to measure the fiber orientation in CFRP laminates from X-ray CT images. In the method, the fiber orientation is analyzed by the application of digital image correlation method (DIC) to the acquired tomographic images. Using DIC, the brightness pattern, which results from the radiodensity difference between fiber and resin, is compared between two different planes in the thickness direction. Then three-dimensional displacement of the brightness pattern, which indicates the fiber orientation, can be measured. This study applied the proposed method to a quasi-isotropic CFRP laminate. After X-ray CT imaging, the sample was sectioned and polished. The fiber orientation was then measured experimentally using microscopy. The fiber orientation calculated using the proposed method agrees very well with the experimentally measured one. After demonstrating the validity of the proposed method, we applied it to a plain woven CFRP laminate. Results revealed that an invalid fiber orientation might be calculated for fibers parallel to the plane of the CT image, or for the fiber orientation of the pattern around the outer edge of CT images.

Key words: microstructures; fiber orientation; x-ray computed tomography; digital image correlation; statistical analysis

1. INTRODUCTION

Carbon fiber reinforced plastics (CFRP) usually contain internal microscopic defects including tow distortion, voids, and resin-rich regions. These defects have various causes such as thermal residual stress [1], out-of-plane stitching [2] or poor resin impregnation during fabrication. Recently, low-cost composite manufacturing techniques such as vacuum-assisted resin transfer molding (VaRTM) [3-5] or Out-of-Autoclave (OoA) prepreg have been studied to apply these techniques to aerospace applications. Compared to autoclave molding, composites produced using low-cost manufacturing techniques tend to contain more microscopic defects. Therefore, observation and evaluation techniques of microscopic defects and their effects on macroscopic material properties are important. An effective method is finite element analysis using a three-dimensional finite element model constructed by stacking microfocus X-ray computed tomographic images, which contain actual microscopic defects.

Material properties of CFRP differ according to their orientation: characteristics along fibers and perpendicular to fibers are greatly different. For this reason, we must infer fiber orientation from X-ray images and consider the actual fiber orientation when generating finite element models. In GFRP, successful generation of a three-dimensional finite element model that reflects the actual fiber orientation has been reported in the literature [6]. However, for CFRP, it is difficult to distinguish fibers from resin clearly on X-ray CT images because carbon fibers and resin have similar radiodensities. Therefore, an X-ray CT-image-based three-dimensional finite element model of CFRP including the actual distribution of carbon fiber orientation has not been reported. Djukic et al. [7–9] improved the contrast between carbon fibers and resin by

impregnating the fibers with the contrast agent, or by coating the carbon fibers with metal. Then they obtained the fiber orientation. Iida et al. [10] coated the short carbon fibers by metal, and they observed fiber orientation. However, these contrast improvement techniques might affect the formation of microscopic defects. For that reason, those methods are unsuitable for model generation. Scott et al. [11] acquired extremely clear section images using synchrotron radiation computed tomography (SRCT), which uses radiation from a synchrotron accelerator instead of a laboratory source. They evaluated the influence of voids on damage. This technique can distinguish fibers from resin, but using a synchrotron accelerator is not easy. Therefore a simpler, more practical technique is demanded.

This report proposes a new method to measure the fiber orientation in CFRP laminates from X-ray CT images. Using the proposed method, the fiber orientation is analyzed by application of digital image correlation (DIC) to acquired X-ray CT images. This paper is organized as follows: Section 2 outlines the proposed method. In section 3, the validity of the proposed method is checked by application of the method to CFRP laminates. Then the acquired fiber orientation distribution is analyzed statistically. In section 4, problems associated with the proposed method are discussed. Conclusions from the present study are presented in the final section.

2. ANALYTICAL METHOD

It is difficult to digitalize fibers clearly from resin based on X-ray tomography because carbon fibers and matrix resin have similar radiodensities. For that reason, in this study, the brightness pattern on the X-ray CT image which results from the arrangement of the fibers and resin is traced. Figure 1 presents the concept of the proposed method: fiber patterns in different cross-sectional images of the CFRP laminate are compared. Then a subset having similar brightness patterns is sought using

DIC. In the DIC calculation, two tomographic images are regarded as virtual surfaces before and after deformation. The in-plane displacement of the subset, which has similar brightness pattern, is calculated between the two surfaces. For Figure 1, the in-plane subset displacement vector is (a, c). The distance between the two sections is b, and the 3D fiber orientation vector of this subset is (a, b, c). In addition, the contrast on the X-ray CT image need not be strong for the proposed method. Even if fiber and resin cannot be digitalized clearly, the brightness pattern can be traced using DIC. Such contrast can be achieved easily using some commercially available X-ray CT systems. It is noteworthy that the brightness patterns must be similar between two tomographic images so that DIC algorithm can trace the patterns. For this reason, the distance between two sections compared using DIC must be small.

3. VALIDATION OF THE PROPOSED METHOD

3.1. Experimental method

To validate the method proposed in section 2, we measured the fiber orientation using CFRP laminates. The quasi-isotropic CFRP laminate stacking configuration of $[45/0/45/90]_{4S}$, using T800S/#3900-2B prepregs (Toray Industries, Inc.), was used for the test. The CFRP was cut to approximately 2 mm × 2 mm × 6 mm using a diamond saw. Tomographic images of CFRP laminates were acquired using a micro-focus X-ray CT device (MicroXCT-200; Carl Zeiss Microscopy GmbH). The X-ray CT imaging was done in the following conditions: the X-ray tube voltage was 20 kV. The current was 196 μA. 6,400 transmission images were obtained by rotating the specimen from -180 deg to +180 deg. Each exposure time was 5 s. These images were combined and reconstructed to produce a 3D image of the sample. After X-ray CT imaging, the acquired CT images were reconstructed (VGStudioMAX2.2; Volume Graphics GmbH).

Then sectional images perpendicular to the nominal fiber orientation were obtained. Resolution of the reconstructed images was 2.91 μm per pixel. Figure 2 portrays two of the reconstructed CT images. Correlation of the brightness pattern of different section images was calculated using DIC. Then the fiber orientations were acquired using the method proposed in section 2. Correlation computations were performed in the following conditions. The subset size was 17 × 17 pixels. The center of the subset was stepped by every 10 pixels. A program developed by Yoneyama et al. [12] for DIC was used for calculation of the correlation between images. Correlation was conducted for every 10 reconstructed CT images. Then the fiber orientation distribution was calculated in layers where the nominal fiber orientations were 45 deg and -45 deg. After X-ray CT imaging, the specimen was molded into epoxy resin and was polished to yield a section micrograph of the section perpendicular to the through-the-thickness direction. Using this section micrograph, fiber orientations were acquired. By comparing the measured fiber orientations to those calculated using the proposed method, the validity of the proposed method was evaluated.

3.2. Results and discussion

Sections labeled ‘a’ and ‘b’ in Figure 2 were chosen for comparing the fiber orientations. Figure 3 presents magnified tomographic images around those sections. The resolution of these section images was 2.91 μm per pixel. The distance between Figure 2(a) and Figure 2(b) was 29.1 μm because those section images were chosen for every ten sections of whole CT images. Figures 4 and 5 portray fiber orientations of sections ‘a’ and ‘b’ projected to planes that perpendicular to the through-the-thickness direction. Section micrographs of approximately the same sections are also shown in Figs. 4 and 5. The area in which vectors are not illustrated represents the area in which the DIC algorithm could not calculate the displacement of the subset because too few

fibers were present, no brightness pattern existed in the subset, or randomness of the fiber arrangement was insufficient. Figures 6 and 7 show each section micrograph superposed by the calculated fiber orientation. According to Figs. 6 and 7, the calculated fiber orientation agreed very well with the measured one except that the part cannot be traced by DIC. This result demonstrates that the proposed method can calculate the correct fiber orientation qualitatively. It is noteworthy that when fiber orientation vectors were superposed onto the section micrograph, they were rotated about 3 deg for section 'a' and about 2 deg for section 'b' because the X-ray CT images and section micrographs were taken from slightly different angles. The mean fiber orientation and standard deviation were acquired using the proposed method. Those measured from section micrographs are presented in Table 1. The calculated and measured mean values were slightly different from one another, but the difference was approximately equal to the angle to which the vectors had been rotated when they were superposed onto the micrograph. Standard deviations agreed well, especially in section 'b'. Therefore, it was concluded that differences of the average resulted from rigid rotation during X-ray CT imaging and from observation using the optical microscope. The discussion presented above demonstrated that, using the proposed method, the fiber orientation was correctly measured directly from X-ray CT images.

3.3. Statistical evaluation of the fiber orientation distribution

The calculated fiber orientation distribution was evaluated statistically on section 'b'. Fiber orientations were calculated at 2,600 points. The result is shown in Figure 8. The curve in Figure 8 is the probability density function of the normal distribution, using the average and deviation calculated using the proposed method. The histogram shape was apparently that of a normal distribution. Therefore, the fiber orientation distribution was tested using a one-sample Kolmogorov–Smirnov test (one-

sample K–S test): a non-parametric method. A test of goodness of fit for a theoretical distribution can be conducted by comparing the cumulative relative frequency of the theoretical distribution and that of the acquired one. Hypotheses used for the test were the following. The null hypothesis was that "The probability distribution of fiber orientations is a normal distribution." The alternative hypothesis was "The probability distribution of fiber orientations differs from that of a normal distribution." A two-sided test with 5% of levels of significance was conducted. Table 2 presents results of the cumulative relative frequency. In the K–S test, the test statistic was the modulus maximal value of difference. Therefore at this time, d_{max} =0.1814 in Table 2. Approximation of the critical value of 5% of levels of significance is 0.0267. Therefore, the test statistic was larger than the critical value. This result rejects the null hypothesis. The test result revealed that the fiber orientation distribution was not a normal distribution in section 'b'.

4. PROBLEMS RELATED TO THE PROPOSED METHOD

4.1. Experimental methods

In section 3, fiber orientations were measured, applying DIC to sections those were perpendicular to the fiber orientation. As described in this section, we attempted to measure the fiber orientation parallel to the section. The two-dimensional woven CFRP laminate, stacking configuration of which was $[0]_{12}$ using IMS60/#133 3K plane woven prepregs (Toho Tenax Co., Ltd.), was used for the test. CFRP was cut to approximately 5 mm × 5 mm × 2 mm. Tomographic images which were perpendicular to the through-the-thickness direction in CFRP laminates were acquired using a micro-focus X-ray CT device (MicroXCT-200; Carl Zeiss Microscopy GmbH). X-ray CT imaging was performed in the following conditions. The X-ray tube voltage was 40 kV; the current

was 200 μA. In all, 3,200 transmission images were obtained by rotating the specimen from -180 deg to +180 deg. Each exposure time was 15 s. These images were combined and reconstructed to produce a stacking image of the sample. At this time, the resolution of acquired images was 1.77 μm per pixel. The acquired images are shown in Figures 9(a) and 9(b). The correlation of the brightness patterns between Figures 9(a) and 9(b) was calculated using DIC. Fiber orientations were acquired using the proposed method. Correlation computations were performed under the following conditions. The subset size was 32 × 32 pixels. The overlap was 50%. Strain Master 8.1.2 (La Vision GmbH) was used for calculations. After X-ray CT imaging, the specimen was molded into epoxy resin and polished to obtain a section micrograph of a section perpendicular to the through-the-thickness direction. Using this section micrograph, the fiber orientation was measured and compared with the fiber orientation calculated using the proposed method.

4.2. Results and discussion

The distance between Figs. 9(a) and 9(b) was 1.77 μm. Figure 10 shows the projected fiber orientation. Figure 11 shows a section micrograph superposed by calculated fiber orientation. Figure 10 reveals that the proposed method can discriminate a resin-rich area because the lengths of vectors are very small. However in tow, there are some parts where the calculated fiber orientations are not correct. The part where the fiber orientation was calculated correctly showed patterns consisting of sections of fibers. At the area where the fiber orientation was nearly parallel to the plane of the tomographic image, the calculated fiber orientation was markedly different from the correct fiber orientation. One reason for those problems is believed to be the algorithm used for tracing patterns. The DIC algorithm was originally designed to trace the displacement of a random pattern on the material surface. Therefore, it was assumed

that patterns on the material surface never vanish. In the proposed method, two cross-sectional CT images are regarded as virtual material surfaces before and after deformation. When there are fibers oriented parallel to the plane, it is possible that not all the fibers appear in both tomographic images. Patterns might not be visible on the next CT image. The proposed method might calculate an invalid fiber orientation in such cases. For the same reason, we must not choose the outer edge of CT images for calculations. It is necessary to choose the direction of CT images so that fiber sections are visible. Regarding the CT image direction, using section images taken from multiple directions, the proposed method can calculate any fiber orientation.

5. CONCLUSIONS

In this paper, we proposed a new method that measures the fiber orientation distribution in CFRP laminates. This method traces the patterns of the brightness. Using this method, the three-dimensional fiber orientation and its distribution of CFRP are calculable solely from CT images. Additionally, we applied the proposed method to plain woven CFRP. Because of the principle of DIC, for an area where there are fibers parallel to the plane or at the area around the edge of CT images, the proposed method cannot calculate the correct fiber orientation. To calculate the fiber orientation correctly, it is necessary to omit those parts from the calculated area. Using section images taken from multiple directions, the proposed method can calculate any fiber orientation.

ACKNOWLEDGMENTS

The authors gratefully acknowledge S. Yoneyama, Associate Professor of Aoyama Gakuin University, for allowing for us to use his DIC programs.

REFERENCES

1. Sorrentino L, Polini W, Bellini, C. To design the cure process of thick composite parts: experimental and numerical results. Adv. Compos. Mater. 2014;23:225–238.
2. Sakai T, Wakayama S, Perez-Pacheco E, Rodriguez-Laviada J, Rios-Soberanis CR. Damage accumulation behavior of non-crimp fabric-reinforced epoxy composite under static and cyclic tensile loading. Adv. Compos. Mater. 2013; 22:281–297
3. Yokozeki T, Kobayashi Y, Aoki T, Yoshida D, Hirata T. VaRTM process of composites using porous mold. Adv. Compos. Mater. 2013; 22:99–107
4. Matsuzaki R, Seto D, Todoroki A, Mizutani Y. In situ void content measurements during resin transfer molding. Adv. Compos. Mater. 2013; 22:239–254
5. Yokozeki T, Yamazaki W, Kobayashi Y. Investigation into property control of VaRTM composites by resin infusion process. Adv. Compos. Mater. 2014; in-print (DOI: 10.1080/09243046.2014.919432)
6. Schell JSU., Renggli M, van Lenthe GH, Müller R, Ermanni P. Micro-computed tomography determination of glass fibre reinforced polymer meso-structure. Compos. Sci. Technol. 2006;66:2016–2022.
7. Djukic LP, Herszberg I, Walsh WR, Schoeppner GA, Prusty BG, Kelly DW. Contrast enhancement in visualisation of woven composite tow architecture using a MicroCT Scanner. Part 1: Fabric coating and resin additives. Composites Part A. 2009;40:553–565.
8. Djukic LP, Herszberg I, Walsh WR, Schoeppner GA, Prusty BG, Kelly DW. Contrast enhancement in visualisation of woven composite architecture using a MicroCT Scanner. Part 2: Tow and preform coatings. Composites Part A. 2009;40:1870–1879.
9. Djukic LP, Herszberg I, Walsh WR, Schoeppner GA, Prusty BG, Kelly DW. Contrast Enhancement of MicroCT Scans to Aid 3D Modelling of Carbon Fibre Fabric Composites. Appl. Compos. Mater. 2013;20:1215–1230.
10. Iida A et al., Observation in widely various the CFRP containing metal-plated carbon fiber as a tracer. Proceedings; 2013 March 4; Kyoto. Japan JCCM-5(2013) (in Japanese)
11. Scott AE, Sinclair I, Spearing SM, Mavrogordato MN, Hepples W. Influence of voids on damage mechanisms in carbon/epoxy composites determined via high resolution computed tomography. Compos. Sci. Technol. 2014;90:147–153.

12. Yoneyama S. Displacement and Strain Measurement Using Digital Image Correlation. Journal of N.D.I. 2010;59:306–310, (in Japanese).

Table 1 Average and standard deviation of measured fiber orientations

Section and method	Average θ[°]	Standard deviation
Section a, DIC	42.83	1.520
Section a, Micrograph	45.69	1.349
Section b, DIC	43.95	1.142
Section b, Micrograph	46.01	1.150

Table 2 Cumulative relative frequency

Fiber orientations [°]	Observed frequency		Relative frequency		Cumulative relative frequency		Difference
	Calculated value	Normal distribution	Calculated value	Normal distribution	Calculated value	Normal distribution	
39	1	0	0.0004	0.0000	0.0004	0.0000	0.0004
40	6	2	0.0023	0.0006	0.0027	0.0006	0.0021
41	7	27	0.0027	0.0103	0.0054	0.0109	0.0055
42	86	199	0.0332	0.0769	0.0386	0.0878	0.0492
43	310	653	0.1196	0.2517	0.1581	0.3395	0.1814
44	1008	937	0.3887	0.3615	0.5469	0.7010	0.1542
45	805	591	0.3105	0.2279	0.8573	0.9289	0.0716
46	270	163	0.1041	0.0630	0.9614	0.9919	0.0305
47	75	20	0.0289	0.0077	0.9904	0.9996	0.0092
48	16	1	0.0062	0.0004	0.9965	1.0000	0.0035
49	9	0	0.0035	0.0000	1.0000	1.0000	0.0000

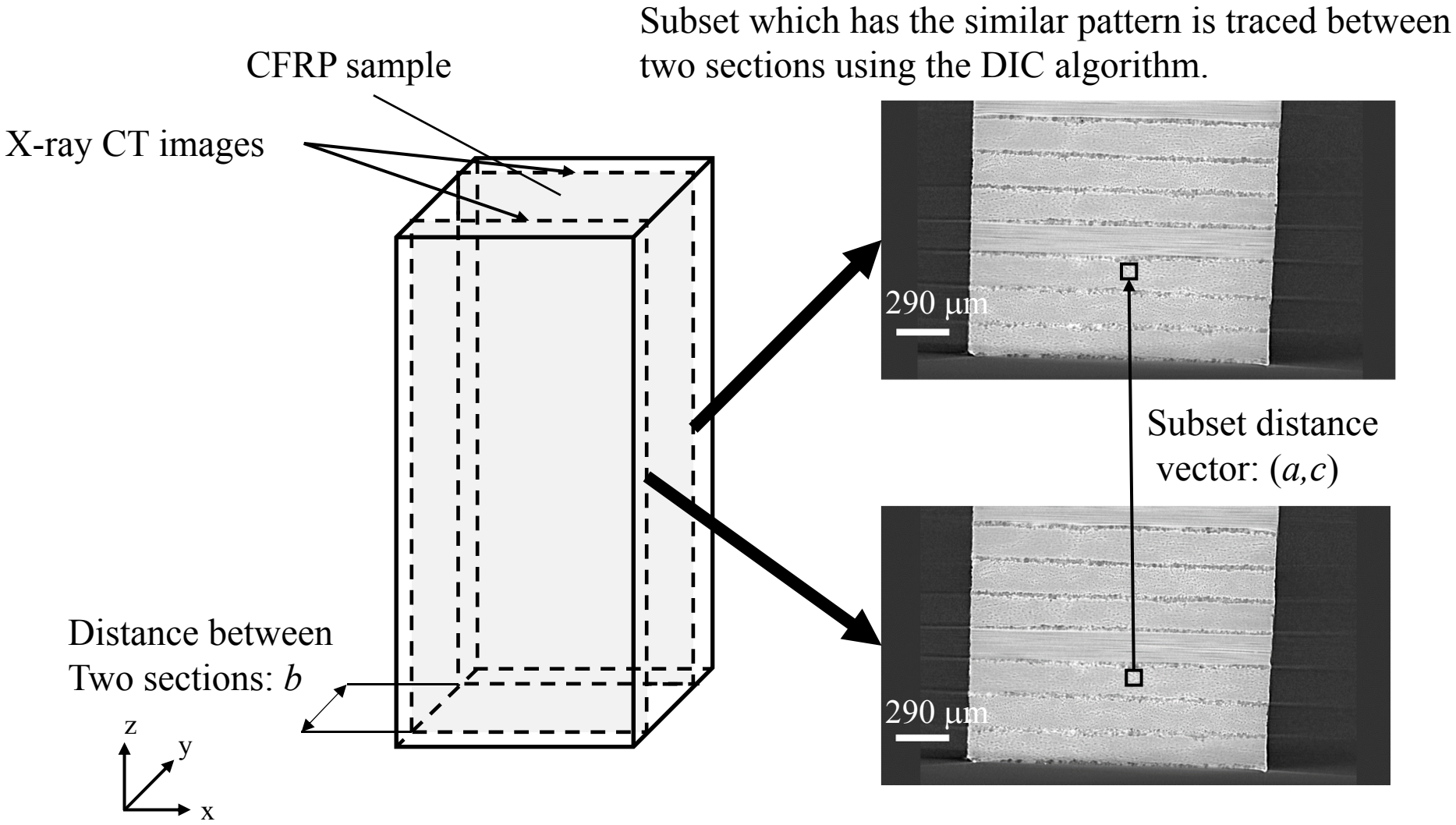

When the subset distance vector is (a,c), 3D fiber orientation vector of this subset is (a,b,c).

Fig. 1 Schematic of the concept of the proposed method.

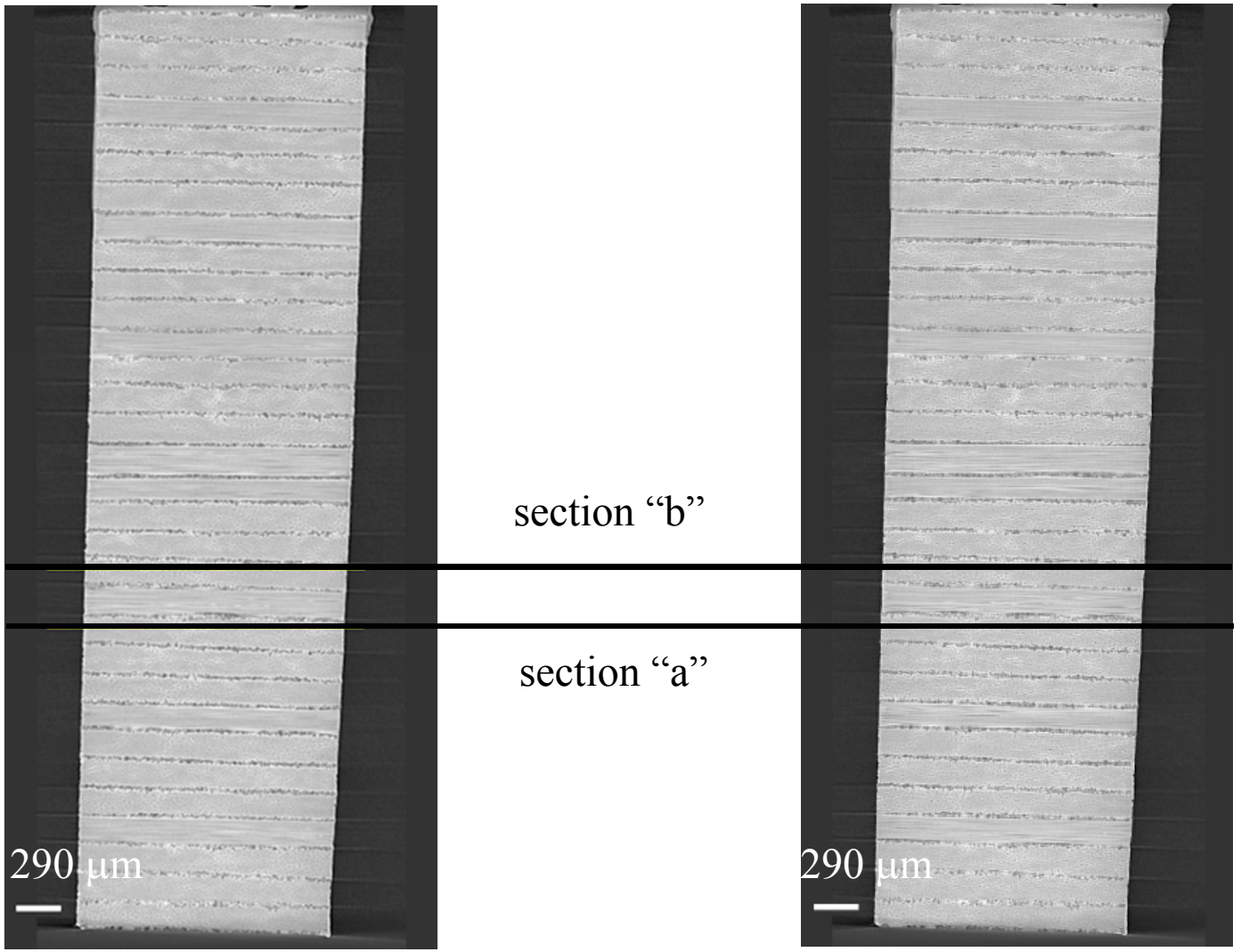

Fig. 2 X-ray CT images

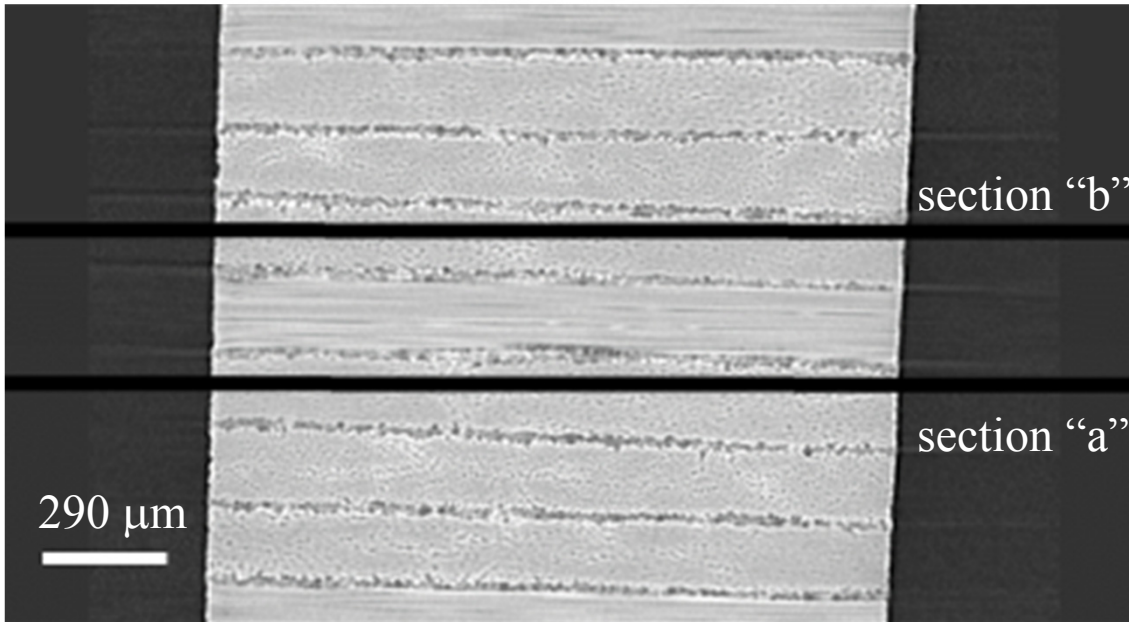

Fig. 3 Magnified view

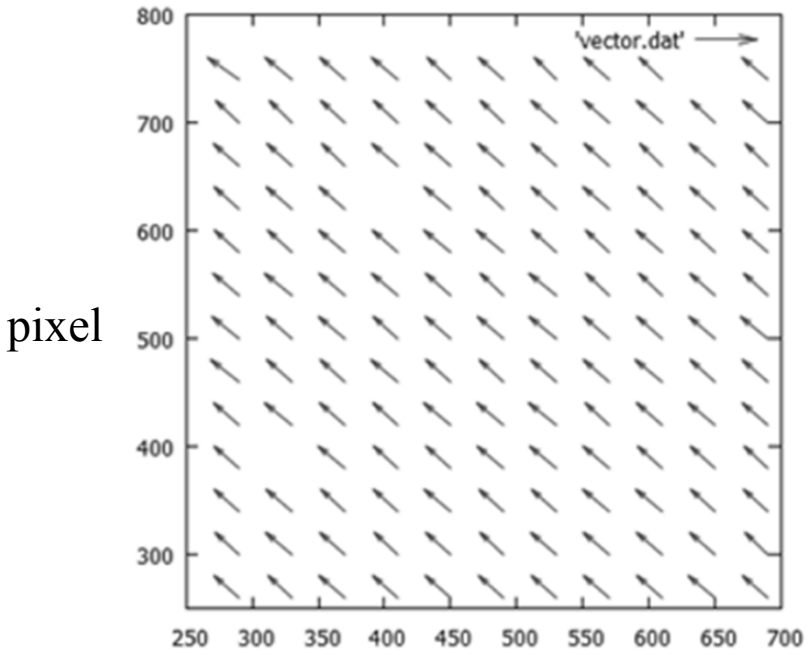

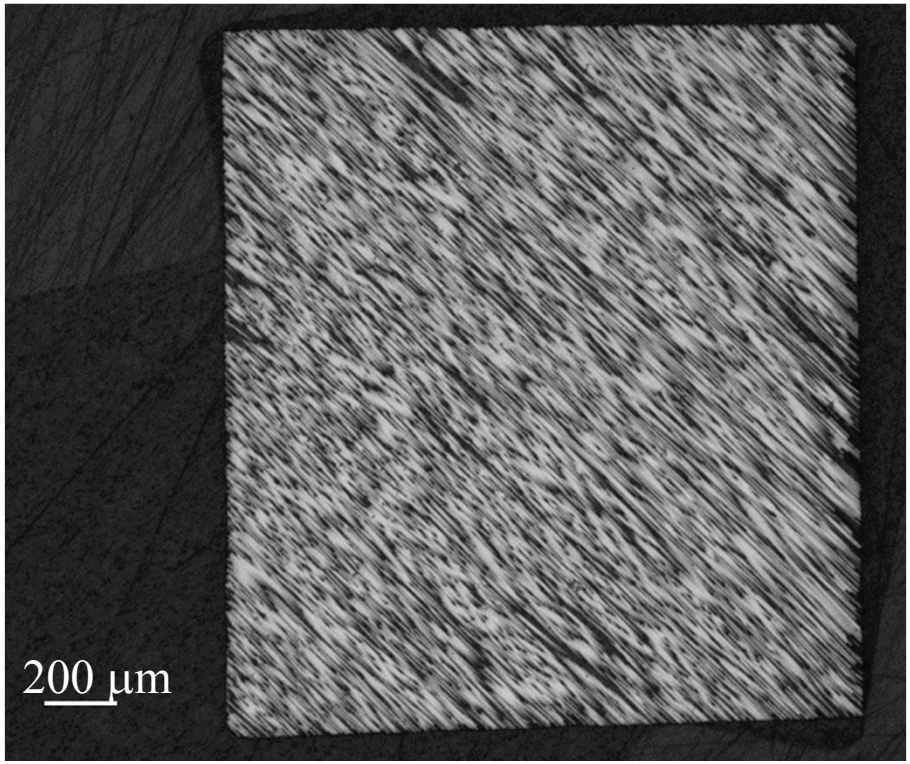

(a) Calculated fiber orientation vectors (b) Section micrograph

Fig. 4 Comparison of fiber orientations on section “a”.

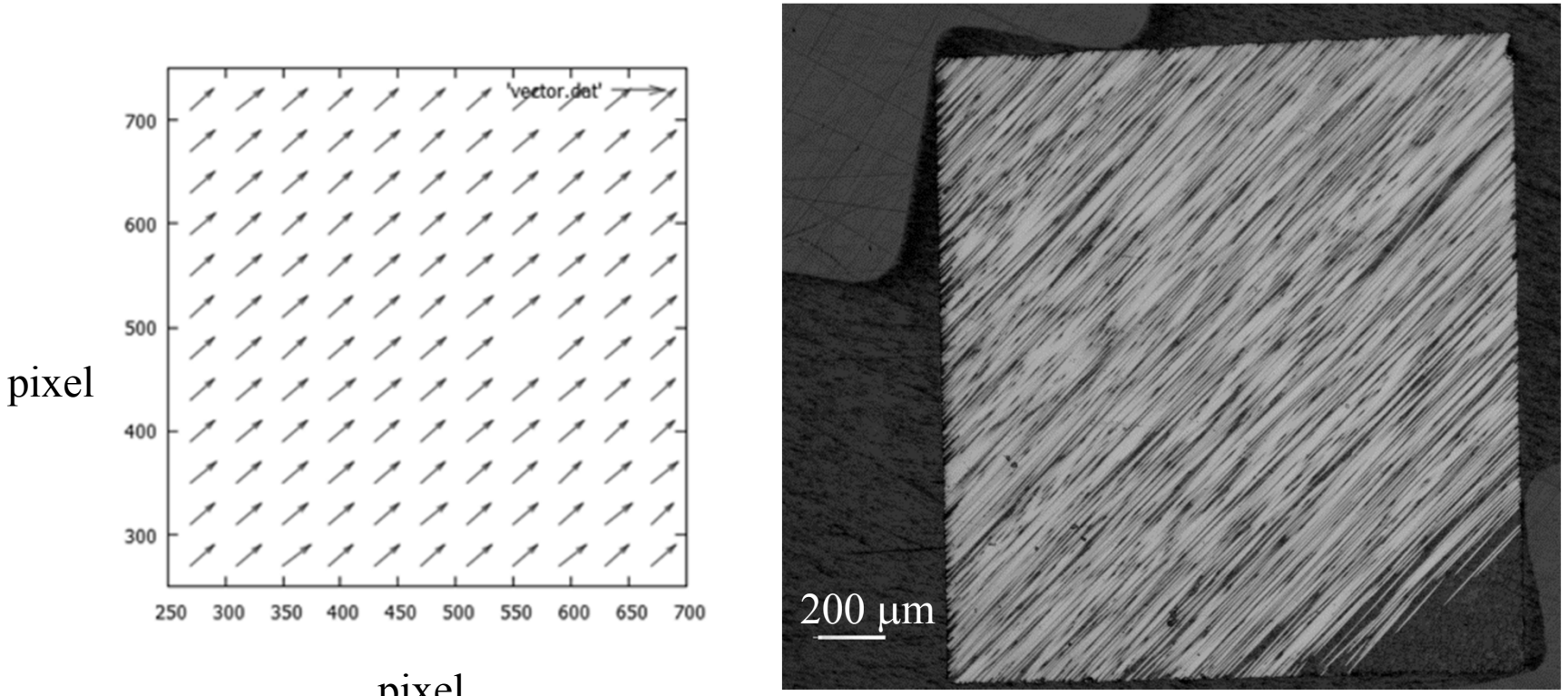

(a) Calculated fiber orientation vectors (b) Section micrograph

Fig. 5 Comparison of fiber orientations on section “b”.

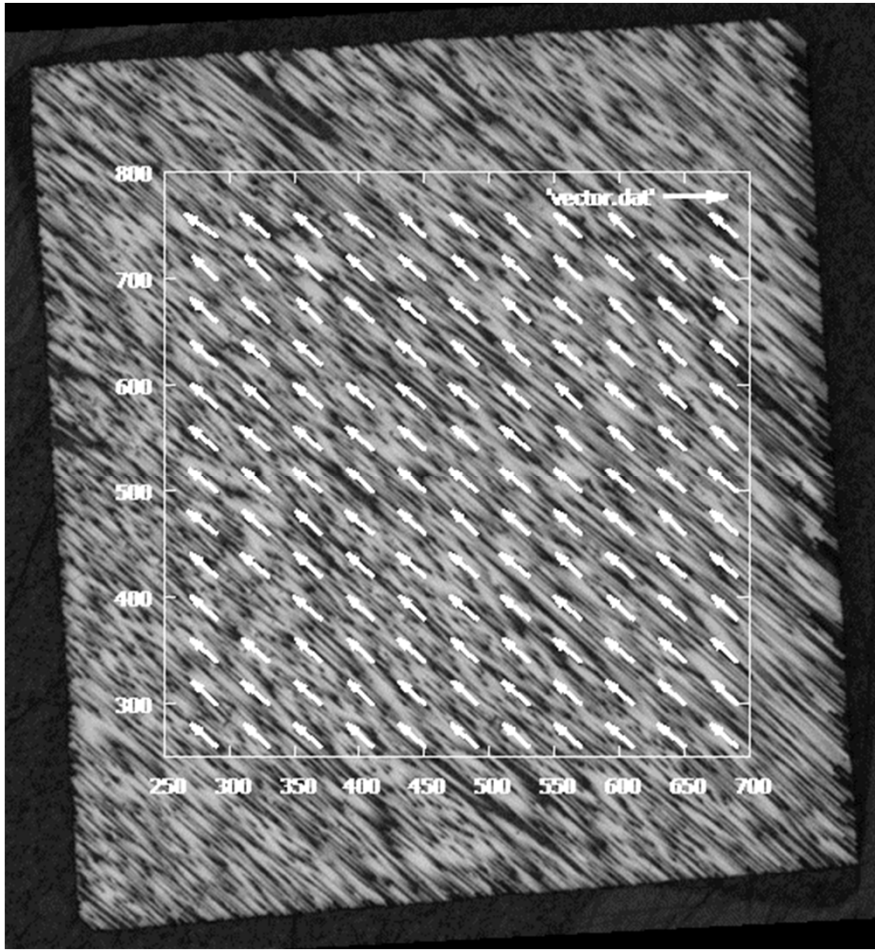

Fig. 6 Section superposed by fiber orientation in section “a”.

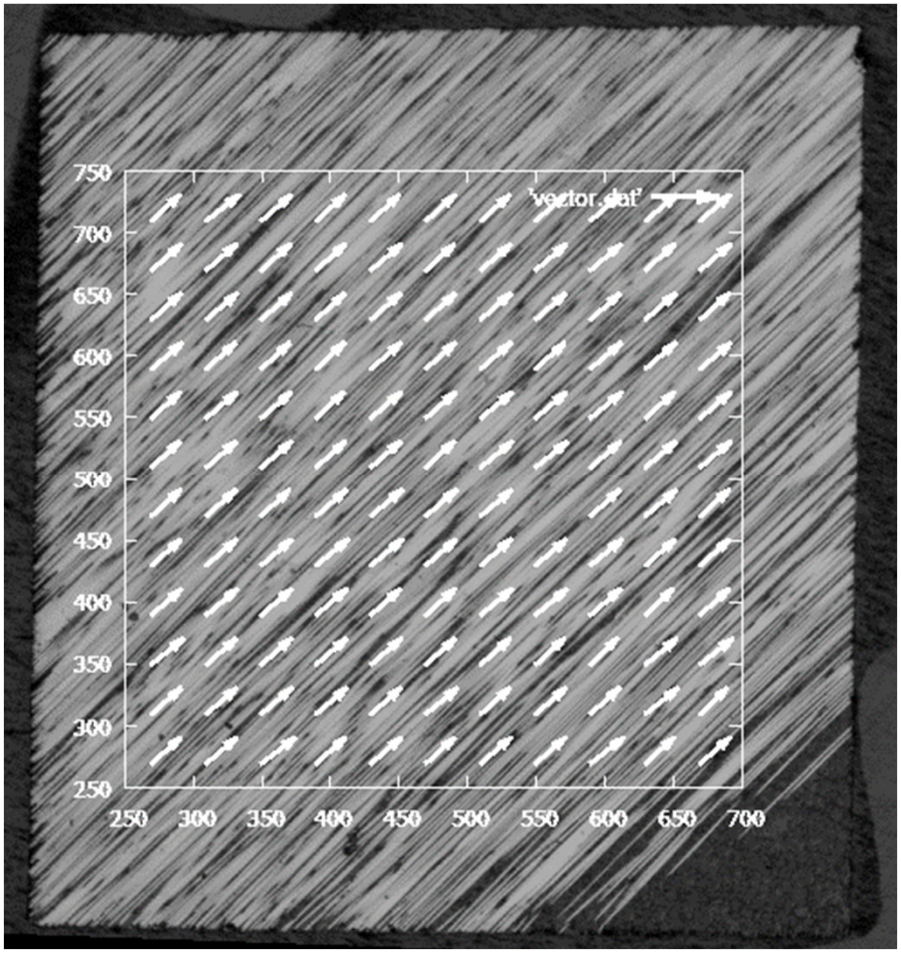

Fig. 7 Section superposed by fiber orientation in section “b”.

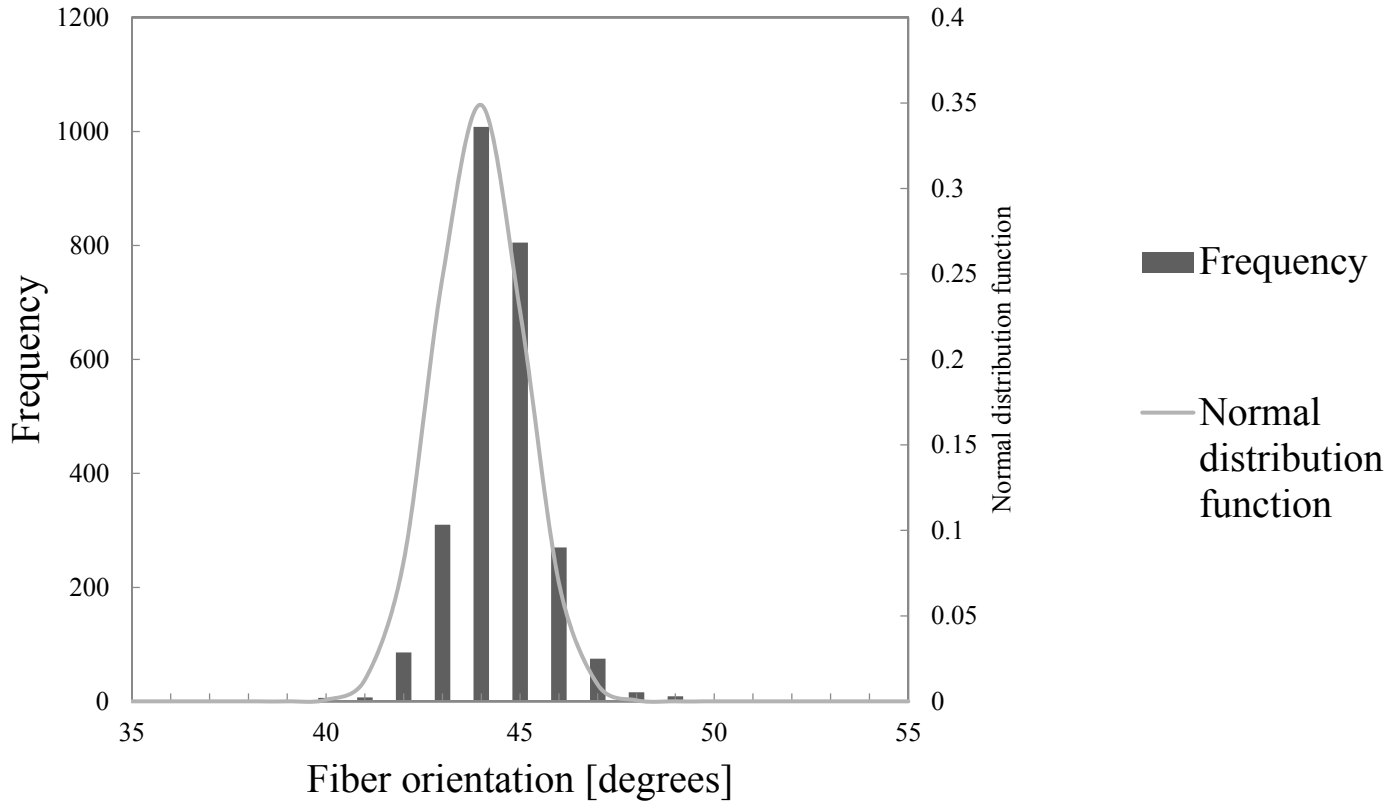

Fig. 8 Comparison between histogram of fiber orientation and normal distribution.

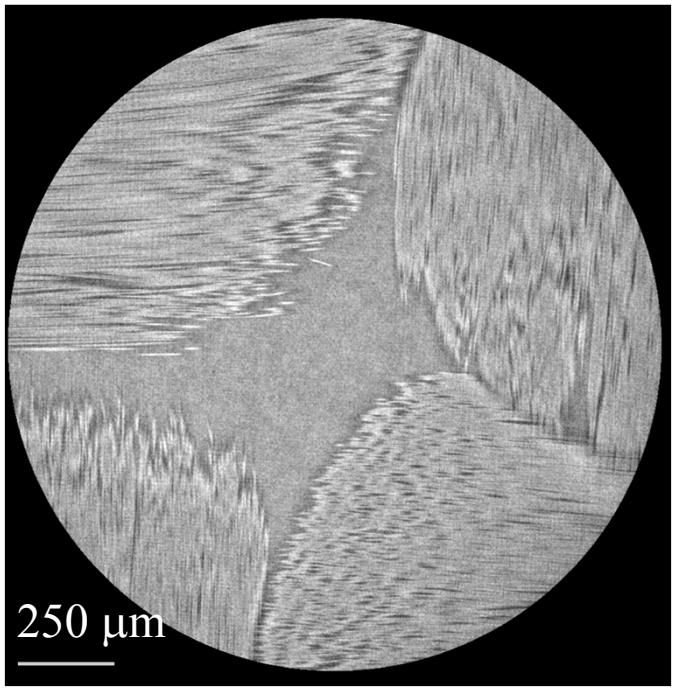

(a)

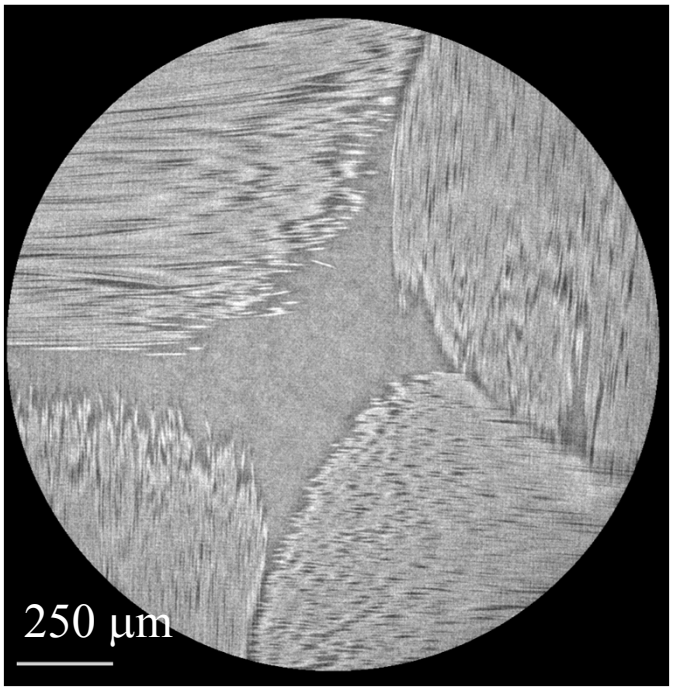

(b)

Fig. 9 X-ray CT images of woven composites.

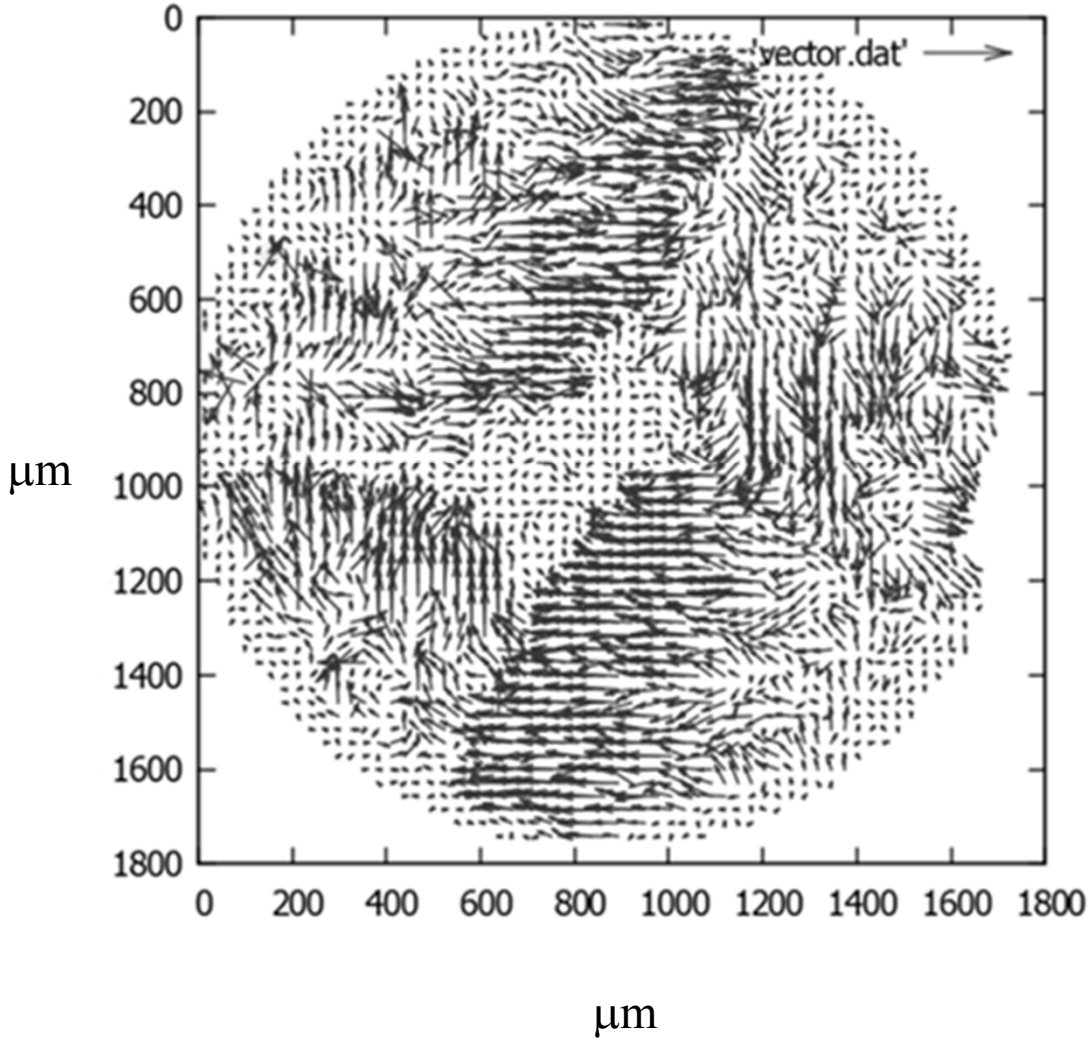

Fig. 10 Fiber orientation vectors.

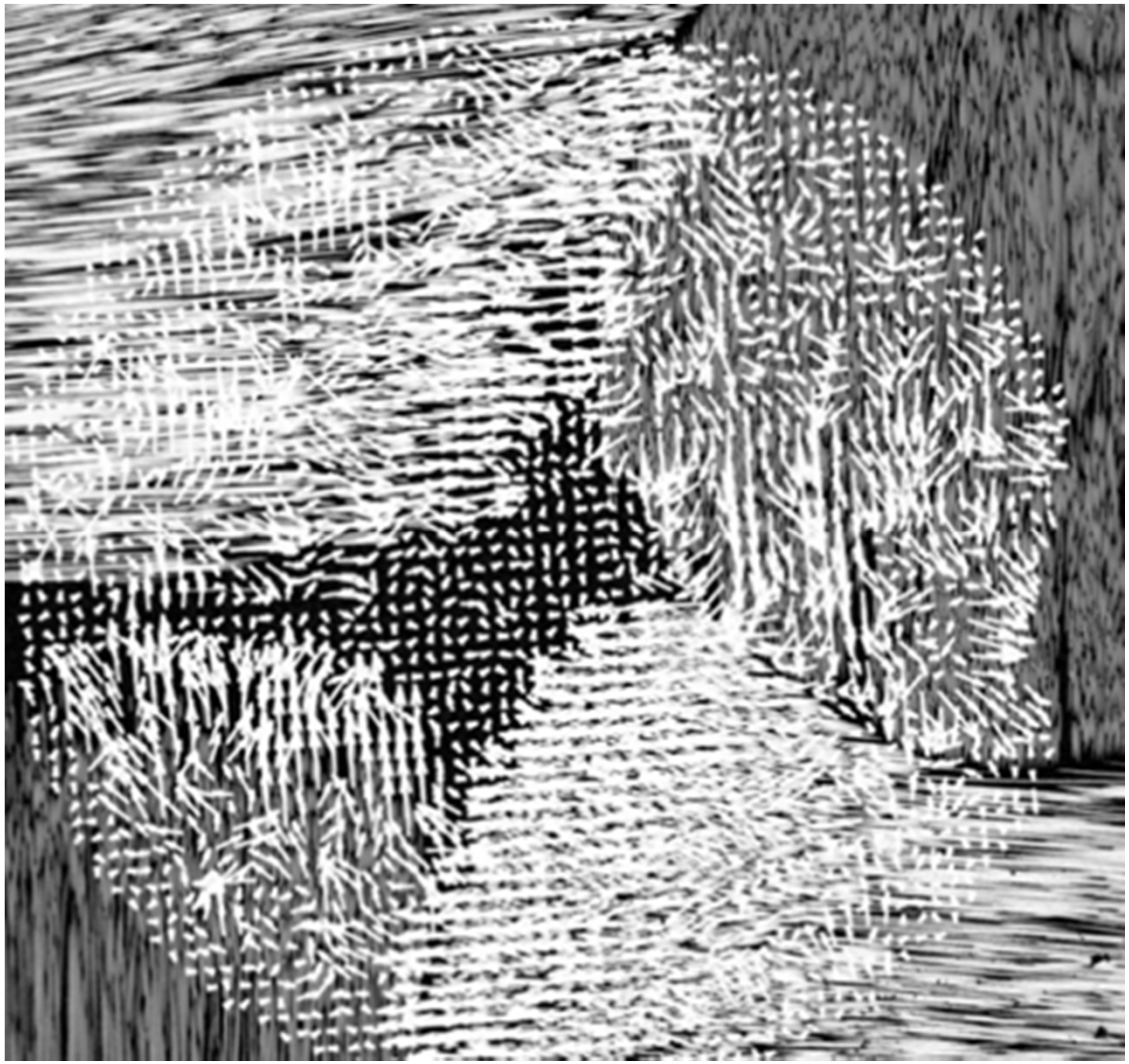

Fig. 11 Section superposed by fiber orientation.